1952

# An experimental analysis of the mixing of a pulsating air jet at varying frequencies in a steady air flow.

Robie, Edgar A.

University of Minnesota

Robie

An experimental analysis of the mixing of a pulsating air jet at varying frequenci in a steady air flow.

# AN EXPERIMENTAL ANALYSIS OF THE MIXING OF A PULSATING AIR JET AT VARYING FREQUENCIES IN A STEADY AIR FLOW

A Thesis

Submitted to the Graduate Faculty

of the University of Minnesota

by

Edgar A. Robie

LCDR, U.S. Navy

In Partial Fulfillment of the Requirements

for the Degree of

Master of Science in Aeronautical Engineering

June 1952

ACKNOWLEDGMENTS

The author wishes to express his appreciation to Dr. Newman A. Hall, Professor Thomas E. Murphy, and Professor Joseph A. Wise for their academic aid; to the Navy group who assisted in operating the equipment and taking the data, and to William Alden and Michael Shonberg for aid in construction of the test apparatus.

It is also desired to thank the U.S. Naval Post-graduate School for sponsoring the attendance of the author at the University of Minnesota for the degree of Master of Science.

TABLE OF CONTENTS

## SUMMARY

The object of this experiment was to investigate the extent of the mixing region of a pulsating air jet at varying frequencies in a steady secondary air flow. This was accomplished by making a velocity survey of the region. The study was made under isothermal conditions at three different frequencies.

The results of this investigation show that the pulsating flow mixes more rapidly and has a shorter potential core than the steady flow jet of the same configuration. Mixing is the best and the potential core is shortest for the pulsating flow at resonant frequency. Decay of the pulsation amplitudes along the centerline is linear. Decay of the pulsation amplitudes laterally is non-linear. The normalized velocity profiles of the pulsating jet downstream from the potential core conform closely to the probability curve.

This test was conducted in the Main Engines Laboratory of the Mechanical Engineering Department at the University of Minnesota, Minneapolis, Minnesota, in partial fulfillment of the requirements for the degree of Master of Science.

# INTRODUCTION

Statement of the Problem:

Many studies, both analytical and experimental, have been made concerning the mixing in fluid streams. The greater majority of these investigations have been limited to free jets and steady flow conditions.

Prandtl's mathematical analysis (1) of mixing length for turbulent flow in free jets as applied by Tollmein (2) along with Taylor's theory (3) have a great utility in studying various types of fluid jet problems. These analyses do not offer a complete explanation of the problem.

Squire and Trouncer (4) have assumed a cosine profile for the normalized velocity and concentration profiles downstream of the potential core. Forstall and Shapiro (5) have deduced several simple empirical formulae for the mixing length downstream of the potential core. The University of Illinois (6) has concluded that the data of free turbulence can be well correlated by probability functions and applied Reichart's Hypothesis to the problem of mixing length.

Little experimental or analytical work has been done in the case of non-stationary flow in which pulsations, either random or regular, exist. The fundamental equations

of fluid motion may be written but remain unsolved since pressure, velocity and temperature are in a continual state of rapid random fluctuations. It is therefore necessary that experimental analyses be made which might introduce techniques to aid in analytical treatment of the problem.

There is a tremendous need for design data concerning the mixing conditions of fuel vapor and air. Consideration has been given to turbulent mixing in free jets and also to jets issuing into ducts. In actual conditions, such as pulsejets, turbojets, ramjets, and combustion chambers, pulsations, both regular and random, do occur. Burton (8) has investigated a very low frequency (250cpm) pulsating jet. In this investigation close agreement was found of the pulsating flow with the steady flow empirical formulae as deduced by Forstall and Shapiro (5).

Godsey and Young (7) state that in gas turbine combustion chambers the most crucial frequencies are in the 6000 cps, 250 to 600 cps, and 25 to 60 cps regions. It has also been found that the critical frequencies in the pulsejet are in the 40 to 300 cps region. This frequency varies with the size of the pulsejet. In ramjets severe pressure and vibrational fluctuations are encountered because of the unsteady nature of the combustion.

Thus, as a second step to that of Forstall and Shapiro (5) it is necessary to introduce pulsations into the flow before the study of actual combustion is introduced.

It is the purpose of this investigation to show the extent of the mixing region of a pulsating air jet at varying frequencies in a steady secondary air flow.

Method of Approach:

Basically the approach to this investigation is experimental in nature. The axial velocity field is plotted from dynamic pressure obtained by making a survey of the mixing region using a total head tube and static pressure tap.

A method of measuring varying dynamic pressures is the Statham Low Range Pressure Transducer. The particular model available for this experiment had a natural frequency of 750 cps. The Strain Analyzer and Brush Recorder units record dynamic pressures up to 100 cps, and direction as well as magnitude of the measured pressure can be read from the chart.

According to Prandtl (1) and Tollmein (2) the static pressure is constant across the jet within small limits. Therefore, a static pressure tap was located in the side of

the test section and used for all points within the flow for each particular lateral traverse.

From the data obtained a comparison of the mixing region of a pulsating jet at varying frequencies, including resonant frequency, may be made with the mixing region of a steady jet.

## TEST EQUIPMENT

General Description:

A schematic diagram of the test equipment is shown in Figure 1. Figures 1a, 1b, 1c, 1d, 1e are photographs of the various component parts of the equipment used.

The apparatus consisted of two separate air supply systems capable of furnishing air to the primary and secondary air flow lines. The primary air flow was obtained from the compressed air line of the building. This system has a capacity of 30 cubic feet at a pressure of 100 p.s.i. The primary air flow into the test apparatus was manually controlled by a two inch gate valve. From the gate valve the air passed through a surge tank ($2\frac{1}{2}$' x 7'), to a 2" standard galvanized pipe which contained a standard A.S.M.E. square edged orifice with "radius" taps as described in (10) for the measurement of the mass rate of flow and a thermocouple upstream of the measuring orifice to measure temperature. The primary air flow was then led into another surge tank ($2\frac{1}{2}$' x 7') and then into a 2" pipe to a rotating type butterfly valve which served as a source of pulsations. From here the air was smoothly reduced to a one inch inside diameter brass tube and ejected into the test section as a free jet. The cylindrical

surge tanks separated the butterfly valve from the measuring orifice to prevent pulsations from traveling upstream to affect the accuracy of the measuring orifice.

The source of secondary air was a gasoline powered Lycoming Model O-435-T air cooled Army tank engine, rated at 162 h.p. at 2800 r.p.m. which drove a centrifugal compressor. The compressor was a 7.48: 1 gear ratio supercharger taken from an Allison V-1710 aircraft engine. The speed of the blower was controlled by throttling the tank engine. The air from the compressor was led to a 6" I.D. smooth black iron pipe, through a measuring orifice as described in (10) into a 22" x 35" steel drum which served as a plenum chamber. This plenum chamber surrounded the primary air flow line. From the plenum chamber the secondary air passed into a square bell with an entrance dimension of 11" x 11" and tapered smoothly to the 6 3/16" square test section. Thus, the secondary air flowed smoothly into the test section and was concentric to the primary air flow. An 18 mesh wire screen was also placed 14" upstream of the flow into the test section to attempt to get small scale turbulence having the same properties in all directions at the test section entrance. A thermocouple was installed in the secondary air line upstream of the orifice to measure temperature of the secondary air.

The test section was an 84" long square (6 3/16" x 6 3/16") duct made of 20 gage sheet metal. One side of the duct was made to slide in sections (14"). The section with the total head tube and static orifice was 4" wide. Thus, this section could be placed in any position along the test duct longitudinally. The downstream end of the duct was open to the atmosphere. A nichrome wire was centered in the test section such that a circuit was completed when the total head tube touched it. This established a reference point for centerline values and the start of lateral traverses.

The total head tube and static pressure orifices were connected to a Statham Low Range Pressure Transducer, Model P6-4D-2100 whose natural frequency was 750 c.p.s. The gage was in turn connected to a Strain Analyzer, Model B1-310, which led to one side of a double pen brush recorder, Model B1-202.

The breaker points mounted on the drive shaft of the pulsator were led to a brush recorder amplifier, Model B1-905, which in turn indicated on the other side of the double pen brush recorder, Model B1-202.

Pulsator:

A 2" diameter disc type butterfly valve rotating

in the primary air flow pipe provided the source of pulsations. When the valve was in the closed position the 2" pipe was completely closed, thus the air flow was varied from zero to maximum. The butterfly valve was driven by a direct drive shaft. This shaft had a standard multiple pulley sheave mounted which was driven through a system of two 6" variable speed pulleys. The variable speed pulley system was driven through a standard multiple pulley sheave which was attached to the shaft of a $\frac{1}{2}$ hp, 110 volt, 1750 r.p.m., A C electric motor. Thus, a wide range of frequencies could be obtained for the pulsation of the primary air flow. A strobotac was used to attain and accurately maintain the desired pulsating frequency.

An eccentric cam was mounted on the pulsator drive shaft which operated a set of breaker points. The breaker points were set to open with the valve in the fully closed position.. In this manner a reference point for valve position was obtained on the brush recorder data.

Instrumentation:

A Kiel type total head tube was used to measure total pressure. The venturi shield surrounding the tube tip to insure flow normal to the tube opening was .375" O.D. . The tube opening was .0625" O.D. and the length of the shaft

to the Statham Low Range Pressure Transducer was 9 inches long with an O.D. of .185". The Kiel tube was mounted in the 4" sliding section of the test duct through a leak proof packing gland. The 4" sliding section also contained a 1/8 inch diameter static orifice.

Water filled manometers were used to measure the differential pressures across the square edged measuring orifices in the 2" and 6" flow lines. Upstream static pressures were measured with mercury filled manometers. The pressure taps from the orifices were located in accordance with A.S.M.E. standards for "radius" taps, (10), the upstream tap being located 1 diameter from the upstream face of the orifice and the downstream tap $\frac{1}{2}$ diameter from the downstream face of the orifice. The static pressure holes were $\frac{1}{4}$" diameter, free of burrs with slightly rounded edges. The orifices were machined to an I.D. of 1.008" and 4.002" for the 2" primary and 6" secondary lines respectively.

Temperatures of the orifices were measured by iron-constantan thermocouples inserted in the flow upstream of the orifices in accordance with A.S.M.E. standards. Temperature readings were made on a Brown potentiometer.

## TEST PROCEDURE

It was necessary to make a static calibration of the Statham Low Range Pressure Transducer using the Strain Analyzer and Brush Recorder instruments. After allowing the instruments time to fully warm up a series of known static pressures were applied to the Statham gage and the deflection read on the Brush Recorder. The scale factor on the Strain Analyzer was also varied from 200 to 50 micro inches per line to obtain the desired range of pressures. Calibration of the Statham pressure gage is shown in Fig. 2. This calibration was used to reduce all data obtained.

All the instrumentation was assembled and checked for leakage and accuracy. Prior to starting a run the tank engine was allowed to warm up as were the Strain Analyzer and breaker point amplifier unit. Zero points were recorded on the Brush Recorder for the various scale settings.

The tank engine which supplied the secondary air flow, was brought up to the desired speed to obtain a velocity of 80 feet per second in the test section. Then the pulsator unit was turned on and checked with the Strobotac at the desired frequency setting. Now the primary air flow was brought to the desired level which was a velocity of

about 160 feet per second at the exit of the 1" brass tube in the test duct.

Brush recorder data was then taken of the various traverses of the total head tube. Lateral traverses were made at a series of stations commencing at the nozzle exit and continued to a distance of 72 nozzle diameters downstream. These lateral traverses commenced with the total head tube on the centerline of the nozzle and continued to a distance of about 2.0" from the centerline.

This type of run was made with the pulsator operating at three frequencies: 1700 r.p.m., 1968 r.p.m., and 2200 r.p.m. The frequency of 1968 r.p.m. was the resonant frequency of the system as found experimentally. A plot of the resonant frequency determination is shown in Fig. 3.

A steady flow run was also made with the pulsator cut off and the butterfly valve secured in the full open position. This was made for comparison with the pulsating runs. The same velocity ratio was held on all the runs. Temperatures and pressures were continually checked on all runs.

## ANALYSIS OF RESULTS

General:

A total of four different runs were made at the same velocity ratio as follows: (1) Steady State; (2) Resonant Frequency---1968 r.p.m.; (3) 2200 r.p.m.; and (4) 1700 r.p.m. The data obtained is listed in Tables I to IV inclusive.

All data obtained from the recording instrumentation was in the form of dynamic pressure (lbs./in.$^2$). This was converted to velocity (ft./sec.) as shown in the section on Sample Calculations. In plotting the data the nozzle exit is taken as the origin of coordinates. The distance along the nozzle centerline is denoted by X/D, positive downstream , in nozzle diameters, Lateral distance from the nozzle centerline is denoted by Y/D. Thus, the station at the nozzle exit is X/D= 0; and the boundary of the nozzle is Y/D = .5.

The resonant frequency of the system was found to be 1968 r.p.m. It was necessary to find this experimentally since the system was between the type which has one end open and one end closed and the type which has both ends open. Calculation provided a starting point for the search of resonant frequency determination. Fig. 3 shows a plot of the

resonant frequency determination. This is not a sharp resonant peak, but one of a damped characteristic.

A butterfly valve provided the source of pulsations in the primary air flow. The primary flow varied from zero to maximum and had a shape similar to that of a harmonic wave.

If flow reversals occurred the total head tube would not have been suitable to use. At no time did the dynamic pressure approach zero on the recording instrumentation, thus, the possibility of flow reversal was discounted.

Steady Flow:

It was desired to compare the mixing region characteristics of the type of flow actually attained with those defined by previous investigations. Forstall and Shapiro (5) have presented several empirical relations for isothermal jet flows similar in nature to this experiment. The following are their conclusions:

(1) "The fully normalized shapes of the velocity and concentration profiles are substantially alike.

(2) The fully normalized shapes of the profiles are substantially independant of velocity ratio and of axial distance.

(3) Beyond the end of the potential core, center-line values of velocity and concentration decrease in inverse proportion to increase in axial distance."

The following empirical relations are based on their experimental data:

(1) X/D value for the end of the potential core:

$$L = 4 + 12\lambda$$

(2) Velocity decay downstream of the potential core. $(X/D > L)$.

$$\frac{U - U_s}{U_p - U_s} = \frac{L}{X/D}$$

Fig. 4 is a plot showing the experimental and theoretical results. Excellent agreement was obtained with the empirical rate of velocity decay. This is indicated by essentially a 1:1 slope of the logarithmic plots. The end of the potential core, "L", is found by the intersection of the straight line velocity plots. Using the empirical formula an L = 9.85 is obtained. This agrees almost exactly with that plotted experimentally.

Normalized velocity profiles are shown in Fig. 9 for the X/D = 11 and X/D = 18 position. This was done by plotting $\frac{U - U_s}{U_c - U_s}$ vs. $r/r_{mv}$. The values of $r_{mv}$ are obtained from Fig. 12 which is a plot of Y/D versus velocity for the particular X/D position. When fully normalized in

this manner, all profiles downstream of the potential core are almost identical for the steady flow case. These profiles have a close resemblance to the cosine curve as found by Squire and Trouncer (4). For direct comparison a cosine curve of the form $\frac{U - U_s}{U_c - U_s} = \frac{1}{2}\left(1 + \cos\frac{\pi r}{2r_{mv}}\right)$ is shown. Good agreement is seen except near the edge of the jet where experimental accuracy in determining $U - U_s$ is not good.

Therefore, with the good agreement from the comparisons with previous acceptable investigations it was thought that the accuracy of measurement and overall experimental accuracy of the test apparatus was sufficient to continue with the pulsating flows.

Pulsating Flow:

The fundamental concern of this investigation was the mixing of a pulsating air jet at varying frequencies in a steady air flow. Three frequencies, resonant (1968 r.p.m.), one above resonance (2200 r.p.m.), and one below resonance (1700 r.p.m.), were used.

Fig. 5 is a plot of the centerline values of the mean velocity for the pulsating flow at 1968 r.p.m. versus the X/D position. It is seen from the comparison with the empirical steady state formula that the potential core is

shortened considerably. The slope of the velocity decay line also differs from the steady state.

A plot of the centerline values of the mean velocity for the pulsating flow at 1700 r.p.m. and 2200 r.p.m. versus X/D position is given in Fig. 6. Here it may be seen that the potential core is shortened, but not as much as that in the resonant frequency case. The slopes of the velocity decay line are approximately the same as that of the resonant frequency run.

The following is a table to enable a better comparison for the pulsating runs with the theoretical steady state case:

| | L | Slope |
|---|---|---|
| Steady State (Theor.) | 9.89 | $L/X/_D$ |
| 1968 r.p.m. | 6.5 | $L/(X/D)^{1.1}$ |
| 1700 r.p.m. | 8.8 | $L/(X/D)^{1.1}$ |
| 2200 r.p.m. | 8.0 | $L/(X/D)^{1.1}$ |

For the steady flow case velocity decay downstream of the potential core ($X/D > L$) is

$$\frac{U - U_s}{U_p - U_s} = \frac{L}{X/D}$$

This empirical formula for the pulsating flow for all frequencies appears to be

$$\frac{U - U_s}{U_p - U_s} = \frac{L}{(X/D)^{1.1}}$$

From the above comparisons it is shown that pulsations shorten the potential core and give faster mixing. Resonant frequency gives the shortest potential core and best mixing.

Plots were also made of the centerline values of the amplitude velocities where the amplitude velocity is the velocity fluctuation computed from the maximum and minimum values of q, versus X/D as shown in Fig. 7 and Fig. 8. The amplitude velocities are expressed in dimensionless form of $\frac{U_{ax} - U_s}{U_a - U_s}$. From these plots it appears that the centerline amplitudes are linear with viscous damping. The slope of the resonant frequency run is less than that of the 1700 r.p.m. and 2200 r.p.m. runs. Using Fig. 7 the equation

$$\frac{U_{ax} - U_s}{U_a - U_s} = e^{-.032\ X/D}$$ for the resonant frequency.

The plot, Fig. 8, for 1700 r.p.m. and 2200 r.p.m. gives a common slope for both frequencies and the equation

$$\frac{U_{ax} - U_s}{U_a - U_s} = e^{-.051\ X/D}.$$

These are the equations for the decay of centerline amplitude velocities in this particular test apparatus. Decay of the resonant frequency run was not as fast as that of the 1700 r.p.m. and 2200 r.p.m. runs.

An attempt was made to do the same with the lateral traverses as was done above with the centerline amplitude velocities. However, these plots were non linear in form. This non linearity probably is caused by the mixing phenomena of the pulsating primary flow and the steady secondary flow.

The data shows a definite phase shift for centerline values of X/D. There also appears to be a phase shift in the lateral traverses made. However, due to insufficient time this phase shift was not recorded. The data also shows that the peak velocity through the butterfly valve did not occur at the full open position. The peak velocity occurred about 10° to 15° from the fully closed position. Apparently here the dynamic pressure was at its highest level.

Again the profiles were made dimensionless and normalized by plotting $\frac{U - U_s}{U_c - U_s}$ versus $r/r_{mv}$. The resulting profile shapes for the pulsating frequencies were compared with the cosine curve, three-halves power curve, and error curve. The curve having the closest resemblence of the above three was that of the error curves. According

to Reichart's Hypothesis (6) data of free turbulence can be correlated by probability functions. Thus, since the pulsating flows investigated in this experiment are closely approximated by the error curve an attempt was made to find the curve which followed the trend of points best. A curve of the form $\frac{U - U_s}{U_c - U_s} = \left[\frac{1}{2}\right] \left(\frac{r}{\bar{r}_{mv}}\right)^{2.4}$ was found to be the one best fitted. This curve is plotted in Figs. 10 and 11, and again it is observed that the points seem to spread near the base of the profile. The experimental accuracy in determining $(U - U_s)$ at the edge of the jet is not too good. The regions which offer the larger pressure differentials give better results than those near the edge of the jet where pressure differentials are smaller.

It is to be noted that the $r_{mv}$ value reverses direction between different X/D stations for each of the four runs made. The $r_{mv}$ value is defined as that radius where the velocity is the arithmetic average of its value on the centerline and in the secondary stream for the particular X/D station. For the steady state run the $r_{mv}$ value reverses between X/D = 24 and X/D = 36. For the pulsating flows the $r_{mv}$ value reverses direction as follows:

Resonant frequency (1968 r.p.m.) --X/D= 15 and X/D = 18

1700 r.p.m.---X/D = 12 and X/D = 15

2200 r.p.m.---X/D = 18 and X/D = 24

Twice the $r_{mv}$ value defines the radius of the outer edge of the velocity profile. The outer edge of the velocity profile never reaches the sides of the test duct.

For the pulsating flows the $r_{mv}$ value reverses direction further downstream as the pulsating frequency increases. The cause for this was not ascertained although it is thought that phase shift might be a contributing factor.

Points at which the centerline flow might be considered mixed to various degrees are shown in the following table. These values are obtained from Figs. 4, 5, and 6. The percent mixing is based on $\left\{1 - \left[\frac{U - U_s}{U_p - U_s}\right]\right\}100$, where $U - U_s$ is the actual velocity gradient which exists at a particular point and $U_p - U_s$ is the maximum velocity gradient which can exist. Thus, the mixing is complete when the fraction $\frac{U - U_s}{U_p - U_s}$ reduces to zero.

| | | 50% | 75% | 90% |
|---|---|---|---|---|
| Steady Flow | X/D = | 19 | 37 | 90 |
| Resonant Frequency (1968 r.p.m.) | X/D = | 10.8 | 19 | 42 |
| 1700 r.p.m. | X/D = | 15.5 | 29 | 66 |
| 2200 r.p.m. | X/D = | 13 | 24 | 54 |

From the above table it is shown that pulsating flow mixes more rapidly than steady flow. It is also seen that at resonant frequency the mixing is accomplished in about one half the distance required by steady flow.

## CONCLUSIONS AND RECOMMENDATIONS

1. The velocity mixing region of an isothermal pulsating jet is much shorter than that of a steady flow jet of the same configuration at the same velocity ratio.

2. Pulsations at the resonant frequency of the test apparatus gives the shortest potential core and the best mixing characteristics. At frequencies above and below resonance the potential core is shorter than the steady flow case and the mixing is better.

3. The centerline velocity, downstream of the potential core, decays in direct proportion to $(X/D)^{1.1}$ for the pulsating flows.

4. The decay of the centerline amplitude velocities appears linear with viscous damping. The decay of the resonant frequency run is not as fast as that of the runs above and below resonance. For the resonant run $\frac{U_{ax} - U_s}{U_a - U_s} = e^{-.032X/D}$ is the equation of the decay.

The equation for the decay above and below resonance is $\frac{U_{ax} - U_s}{U_a - U_s} = e^{-.051\ X/D}$. Decay of the lateral traverses for all pulsating runs was non-linear.

5. The normalized velocity profiles downstream of the potential core are essentially of the same shape, irrespective of the X/D position. They closely resemble the probability curve more so than the cosine or three halves power curve. A curve of the form $\frac{U - U_s}{U_c - U_s} = \left[\frac{1}{2}\right]\left(\frac{r}{r_{.5V}}\right)^{2.4}$ fits the points well.

6. Good agreement was obtained with the findings of Forstall and Shapiro for the steady flow case. The location of the potential core is closely defined by the empirical relation $L = 4 + 12\lambda$. The centerline velocity, downstream of the potential core, decays in direct proportion to X/D. The normalized velocity profiles closely resemble a cosine curve.

7. The centerline flow was considered 90% mixed at X/D positions of 90 for steady flow, 42 for resonant frequency, 66 for 1700 r.p.m., and 54 for 2200 r.p.m. There

was 75% mixing at X/D positions of 37 for steady flow, 19 for resonant frequency, 29 for 1700 r.p.m., and 24 for 2200 r.p.m.

8. With respect to the test apparatus, it is recommended that a surge tank be placed in the secondary air line. Small amplitude pulsations were noted on the recording data which were traced to the blower operated by the tank engine.

9. Further investigations of this nature are recommended to find the effects of phase shift, pulsation form and velocity ratio upon the mixing region of a pulsating jet. Phase shift is apparent and readable to a low degree of accuracy on the data obtained. It is thought that photographs of an oscilloscope screen might provide readable data.

## FORMULAS AND SAMPLE CALCULATIONS

1. Air Flow Measurement and Calculation

The equation used to find mass flow was:

$$W = 0.688\ A_2\ \text{Key}\ (\rho \Delta p)^{\frac{1}{2}}$$

(see Ref. 10)

2. Calculation of Reynolds Number

$$N_R = \frac{\rho u D}{A}$$

3. Frequency Computations

The natural frequency of the tube with one end closed is computed from

$$f = \frac{a}{4L}$$

The natural frequency of the tube with both ends open is computed from

$$f = \frac{a}{2L}$$

4. Calculation of velocity

$$p = \rho RT$$

where $p = 2116$ lbs./ft$^2$
$R = 1715$ ft$^2$/sec$^2$ °R
$T = 565°$ R

$$\rho = \frac{2116 \text{ lbs./ft}^2}{(1715 \text{ ft}^2/\text{sec}^2\,°\text{R})(565°\text{R})} = .00218 \text{ slugs/ft}^3$$

$q = \frac{1}{2}\rho V^2$

where $\rho$ = .00218 slugs/ft$^3$

q = Dynamic Pressure lbs./in.$^2$

$$V^2 = \frac{2q}{\rho} = \frac{(2)(144\ in^2/ft^2)(\ q\ lbs./in^2)}{.00218\ slugs/ft^3}$$

$$V^2 = 132 \times 10^3\ q\ \frac{ft^2}{sec^2}$$

$$V = 363.5\ \sqrt{q}\ \ ft/sec.$$

## NOMENCLATURE

D ..... diameter of primary jet nozzle, inches.

L ..... value of X/D for end of potential core.

r ..... radial distance from jet axis.

q ..... dynamic pressure, psi.

$r_{mv}$.... radius where velocity is arithmetic average of its value on the axis and in secondary stream, for a given X.

U..... time average velocity in axial direction.

$U_c$..... velocity on axis at a given X.

$U_p$ .... velocity of primary stream at X = 0.

$U_s$ .... velocity of undisturbed secondary stream.

$U_a$ .... velocity of pulsation amplitudes on the axis at X = 0.

$U_{a_x}$ ... velocity of pulsation amplitudes on the axis at a given X.

X ..... axial distance downstream from nozzle exit, inches.

Y ..... lateral distance from nozzle centerline, inches.

$\lambda$ ..... velocity ratio. $U_s/U_p$.

$\rho$ ..... density

$\mu$ ..... viscosity

BIBLIOGRAPHY

(1) PRANDTL, L.; "Report on the Investigation of Developed Turbulence"; NACA T. M. 1231, September 1949.

(2) TOLLMIEN, W.; "Calculation of Turbulent Expansion Processes"; NACA T. M. 1085, 1945.

(3) TAYLOR, G. I.; "The Transport of Vorticity and Heat Through Fluids in Turbulent Motion"; Proc. Roy. Soc.A135, p. 685 and 702, 1932.

(4) SQUIRE and TROUNCER; "Round Jets in a General Stream"; R and M 1974, British ARC, 1944.

(5) FORSTALL and SHAPIRO; "Momentum and Mass Transfer in Coaxial Gas Jets"; Journal of Applied Mechanics, vol. 17, No. 4, December 1950.

(6) ALEXANDER, BARON, CUMMINGS; "Transport of Momentum, Mass, and Heat in Turbulent Jets" Part I, Engineering Experiment Station, University of Illinois Technical Report No. 8, September, 1950.

(7) GODSEY and YOUNG; "Gas Turbines for Aircraft"; p. 152, McGraw-Hill, 1949.

(8) BURTON, C. J.; "Preliminary Investigation of the Mixing of a Pulsating Air Jet in a Steady Secondary Air Flow", Masters Thesis, University of Minnesota, August 1951.

(9) KNOTTAGE, H. B.; "Turbulence-Fundamental Frontier in Air Flow"; Heating, Piping, and Air Conditioning, pp. 115-122, April 1949.

(10) "Flow Measurement", 1949, A.S.M.E. Power Test Code 19.5; 4-1949.

# APPENDIX

TABLE I

STEADY FLOW CENTERLINE VELOCITIES

$U_p$ = 160ft/sec; $U_s$ = 78 ft/sec; $\lambda$ = .487

| $\frac{X}{D}$ | Scale Factor | Deflection (m.m.) | q lbs/in.$^2$ | $U^2 \times 10^3$ ft$^2$/sec$^2$ | U ft/sec | $\frac{U - U_s}{U_p - U_s}$ |
|---|---|---|---|---|---|---|
| 0 | 100 | 8.8 | .195 | 25.2 | 159.1 | |
| 3 | 100 | 9.2 | .205 | 26.4 | 162.0 | 1.025 |
| 6 | 100 | 8.7 | .194 | 25.0 | 158.1 | .98 |
| 7 | 100 | 9.0 | .200 | 25.8 | 160.5 | 1.005 |
| 8 | 100 | 8.5 | .190 | 24.5 | 156.6 | .96 |
| 9 | 100 | 8.6 | .191 | 24.6 | 157.0 | .964 |
| 10 | 100 | 7.3 | .162 | 20.9 | 144.5 | .935 |
| 11 | 100 | 6.9 | .154 | 19.88 | 141.0 | .89 |
| 12 | 100 | 6.3 | .140 | 18.10 | 134.8 | .694 |
| 15 | 100 | 5.2 | .115 | 14.82 | 121.9 | .535 |
| 18 | 50 | 8.3 | .107 | 13.8 | 117.5 | .482 |
| 24 | 50 | 7.0 | .091 | 11.72 | 108.1 | .367 |
| 36 | 50 | 6.3 | .082 | 10.59 | 103.0 | .305 |
| 48 | 50 | 5.3 | .069 | 8.90 | 94.5 | .201 |
| 60 | 50 | 5.4 | .070 | 9.03 | 95.1 | .208 |
| 72 | 50 | 5.4 | .070 | 9.03 | 95.1 | .208 |

TABLE II

STEADY FLOW LATERAL TRAVERSE FOR X/D = 11

$U_p$ = 160 ft/sec; $U_c$ = 141 ft/sec; $U_s$ = 78 ft/sec; $\lambda$ = .487

$r_{mv}$ = .42"

| $\frac{Y}{D}$ | Scale Factor | Deflection (m.m.) | q lbs/in$^2$ | $U^2 \times 10^3$ ft$^2$/sec$^2$ | U ft/sec | $\frac{r}{r_{mv}}$ | $\frac{U - U_s}{U_c - U_s}$ |
|---|---|---|---|---|---|---|---|
| 0 | 100 | 6.9 | .154 | 19.88 | 141.0 | 0 | 1 |
| .1 | 100 | 6.7 | .150 | 19.35 | 139.0 | .238 | .959 |
| .2 | 100 | 6.3 | .140 | 18.05 | 134.5 | .475 | .850 |
| .3 | 100 | 5.6 | .125 | 16.11 | 127.0 | .714 | .70 |
| .4 | 50 | 8.7 | .113 | 14.60 | 121.0 | .955 | .57 |
| .5 | 50 | 7.8 | .100 | 12.90 | 113.8 | 1.19 | .415 |
| .6 | 50 | 7.3 | .095 | 12.25 | 110.8 | 1.43 | .35 |
| .8 | 50 | 5.8 | .075 | 9.69 | 98.1 | 1.90 | .077 |
| 1.0 | 50 | 5.4 | .071 | 9.15 | 96.6 | | |
| 1.2 | 50 | 5.3 | .069 | 8.90 | 94.5 | | |
| 1.4 | 50 | 5.3 | .069 | 8.90 | 94.5 | | |
| 1.6 | 50 | 5.2 | .068 | 8.77 | 93.5 | | |

TABLE III

PULSATING FLOW CENTERLINE MEAN AND AMPLITUDE VELOCITIES

RESONANT FREQUENCY - 1968 r.p.m.

$U_p$ = 158 ft/sec; $U_s$ = 77.5 ft/sec; $\lambda$ = .49

| $\frac{X}{D}$ | Scale Factor | $P_B$ (m.m.) | $P_A$ (m.m.) | $q_B$ lb/in$^2$ | $q_A$ lb/in$^2$ | $U_B$ ft/sec | $U_A$ ft/sec | $\frac{U-U_s}{U_p-U_s}$ | $\frac{U_{ex}-U_s}{U_a-U_s}$ |
|---|---|---|---|---|---|---|---|---|---|
| 0 | 200 | 4.5 | 11.0 | .195 | .477 | 160 | 251 | --- | --- |
| 3 | 200 | 4.1 | 9.5 | .180 | .412 | 154.5 | 235 | .959 | .91 |
| 6 | 200 | 4.0 | 9.0 | .175 | .390 | 152 | 227 | .927 | .865 |
| 7 | 200 | 3.5 | 8.5 | .153 | .370 | 142.1 | 221 | .804 | .825 |
| 8 | 200 | 3.2 | 8.0 | .140 | .348 | 136 | 214.5 | .727 | .79 |
| 9 | 200 | 2.8 | 7.8 | .124 | .339 | 128 | 212 | .628 | .775 |
| 10 | 200 | 2.5 | 7.0 | .108 | .304 | 119.5 | 200 | .521 | .706 |
| 11 | 200 | 2.3 | 7.0 | .100 | .304 | 115 | 200 | .465 | .706 |
| 12 | 200 | 2.15 | 6.3 | .093 | .274 | 111 | 190.5 | .416 | .651 |
| 15 | 200 | 1.85 | 6.0 | .080 | .260 | 103 | 185 | .316 | .62 |
| 18 | 200 | 1.70 | 4.4 | .075 | .191 | 99.5 | 159 | .274 | .47 |
| 24 | 200 | 1.45 | 3.8 | .064 | .166 | 92 | 148 | .180 | .405 |
| 36 | 100 | 2.6 | 3.1 | .057 | .070 | 87 | 96 | .118 | .107 |
| 48 | 100 | 2.4 | | .055 | | 85.2 | | .096 | |
| 60 | 50 | 4.0 | | .051 | | 82.1 | | .057 | |
| 72 | 50 | 4.0 | | .051 | | 82.1 | | .057 | |

TABLE IV

PULSATING FLOW LATERAL TRAVERSE FOR X/D = 11

RESONANT FREQUENCY - 1968 r.p.m.

$U_p$ = 158 ft/sec; $U_c$ = 115 ft/sec; $U_s$ = 77.5 ft/sec

$\lambda$ = .49; $r_{mv}$ = .48

| $\frac{Y}{D}$ | Scale Factor | Deflection (m.m.) | q lbs/in$^2$ | U ft/sec | $\frac{r}{r_{mv}}$ | $\frac{U - U_s}{U_c - U_s}$ |
|---|---|---|---|---|---|---|
| 0 | 200 | 2.3 | .100 | 115 | 0 | 1 |
| .1 | 200 | 2.25 | .097 | 113 | .208 | .947 |
| .2 | 100 | 4.15 | .092 | 110 | .416 | .868 |
| .3 | 100 | 3.9 | .086 | 106.5 | .625 | .774 |
| .4 | 100 | 3.6 | .080 | 102.6 | .833 | .670 |
| .5 | 100 | 3.0 | .066 | 93.5 | .960 | .426 |
| .6 | 100 | 2.5 | .055 | 85.1 | 1.25 | .202 |
| .8 | 100 | 2.1 | .047 | 79.0 | 1.66 | .04 |
| 1.0 | 100 | 2.0 | .045 | 77.2 | 2.08 | 0 |
| 1.2 | 100 | 2.1 | .047 | 79.0 | | |
| 1.4 | 100 | 2.0 | .045 | 77.2 | | |
| 1.6 | 100 | 2.0 | .045 | 77.2 | | |
| 1.8 | 100 | 2.0 | .045 | 77.2 | | |

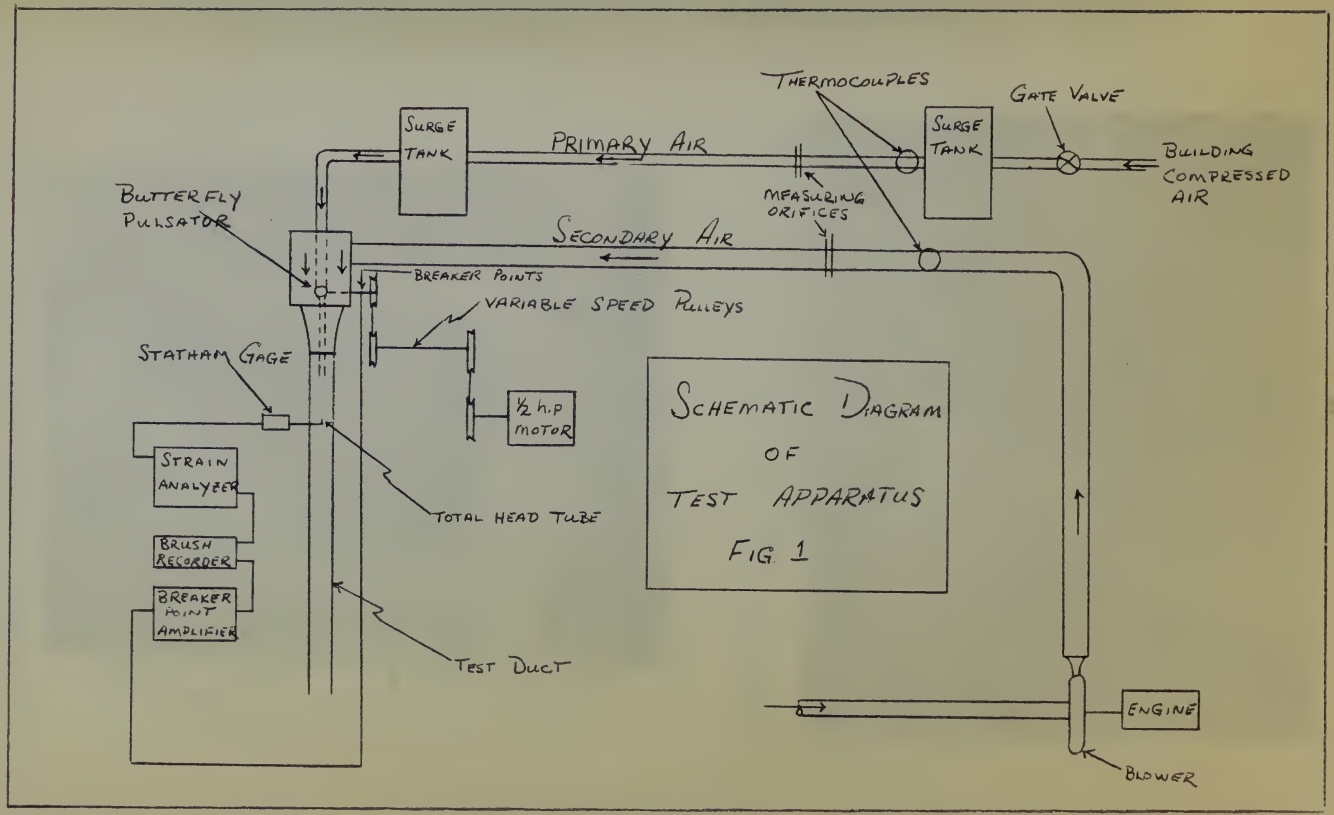


SCHEMATIC DIAGRAM OF TEST APPARATUS

FIG. 1

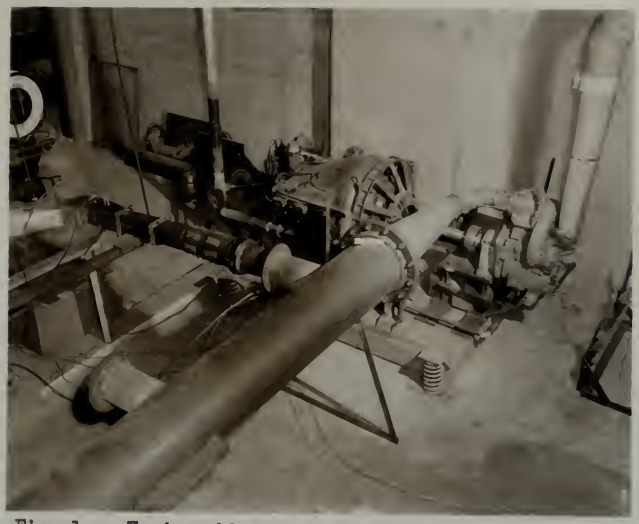

Fig. 1-a Engine, blower, and manifold.
(The test set-up shown is not part of this experiment)

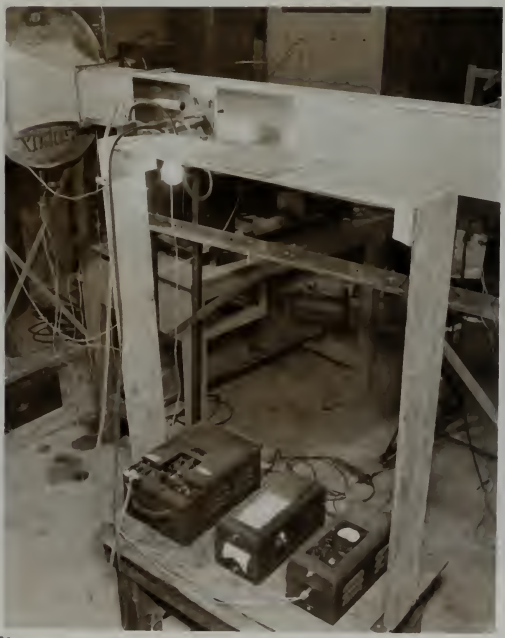

Fig. 1-b Test duct and recording instrumentation.

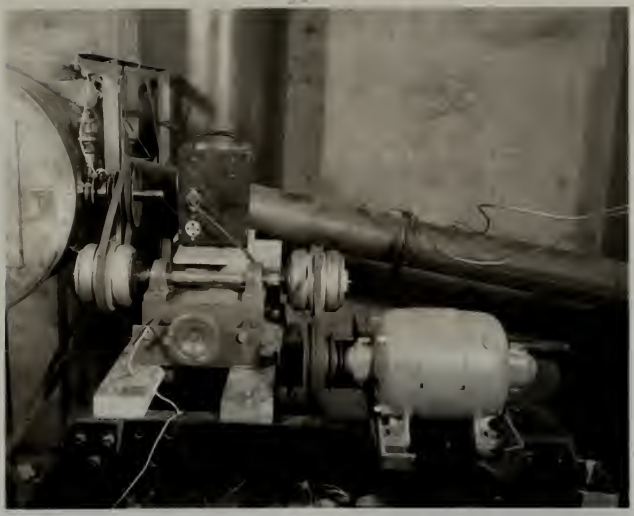

Fig. 1-c Pulsator Unit

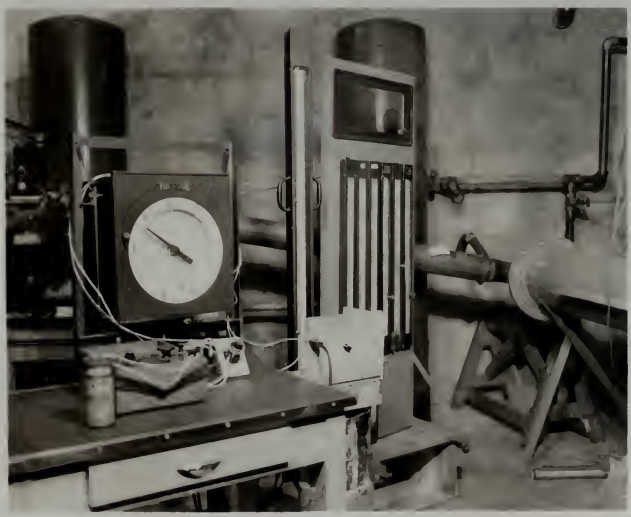

Fig. 1-d Controlling instrumentation.

Fig. 1-e Control panel for engine operation.

# Calibration of Statham Transducer

Fig. 2

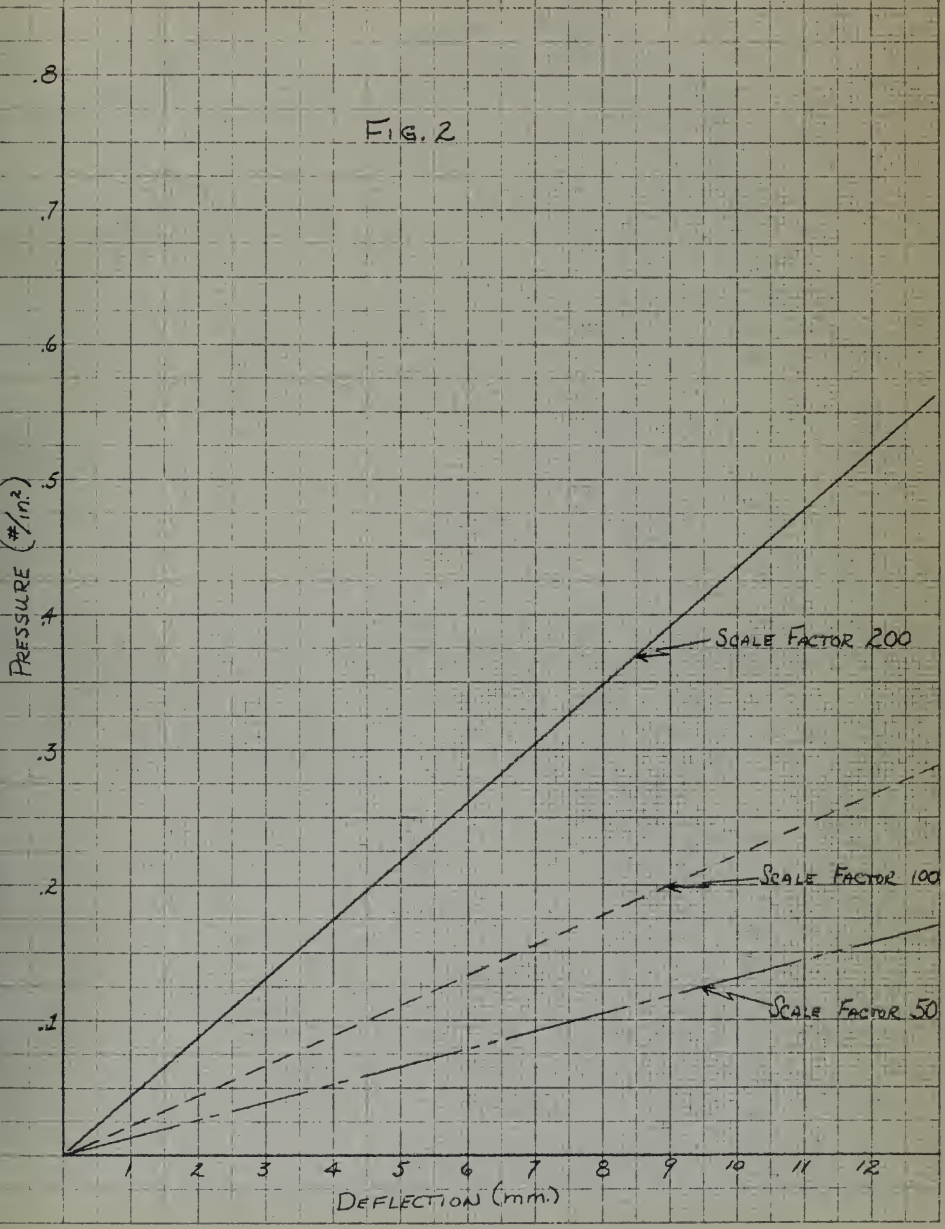

# EXPERIMENTAL RESONANT FREQUENCY CURVE

FIG. 3

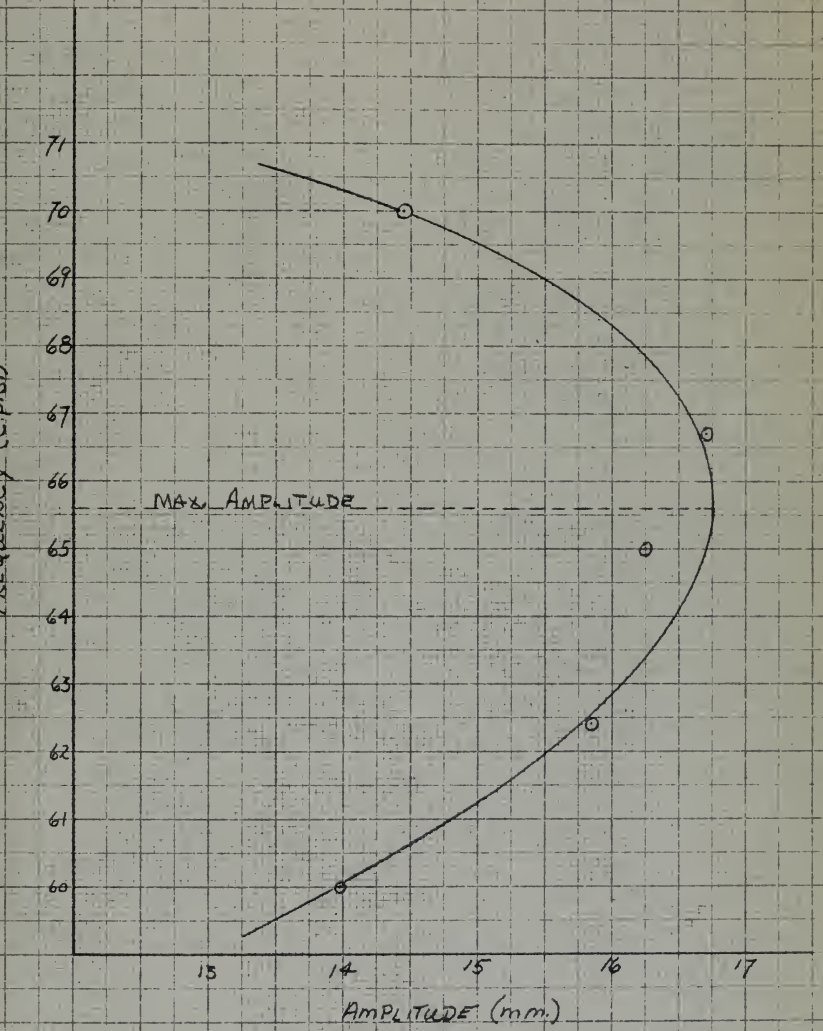

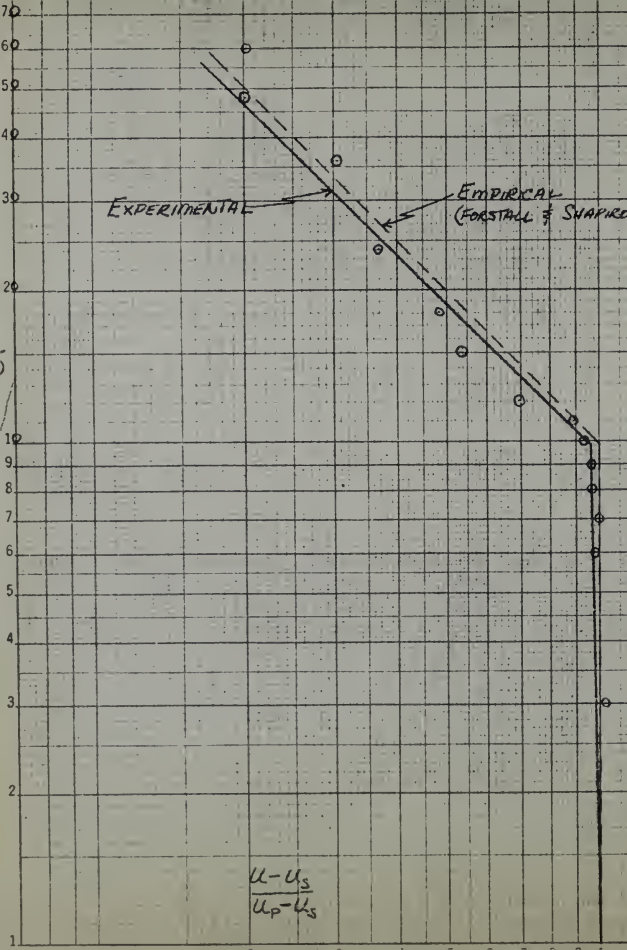


CENTERLINE VALUES OF VELOCITY

FOR STEADY FLOW

$\lambda = .487$

FIG. 4

EMPIRICAL EQUATIONS:

$L = 4 + 12\lambda = 9.85$

$\frac{u+u_s}{u_p-u_s} = \frac{L}{x/D}$ (FOR $\frac{x}{D} > L$)

CENTERLINE VALUES OF VELOCITY

PULSATING FLOW - RESONANT FREQUENCY - 1968 R.P.M.

FIG. 5

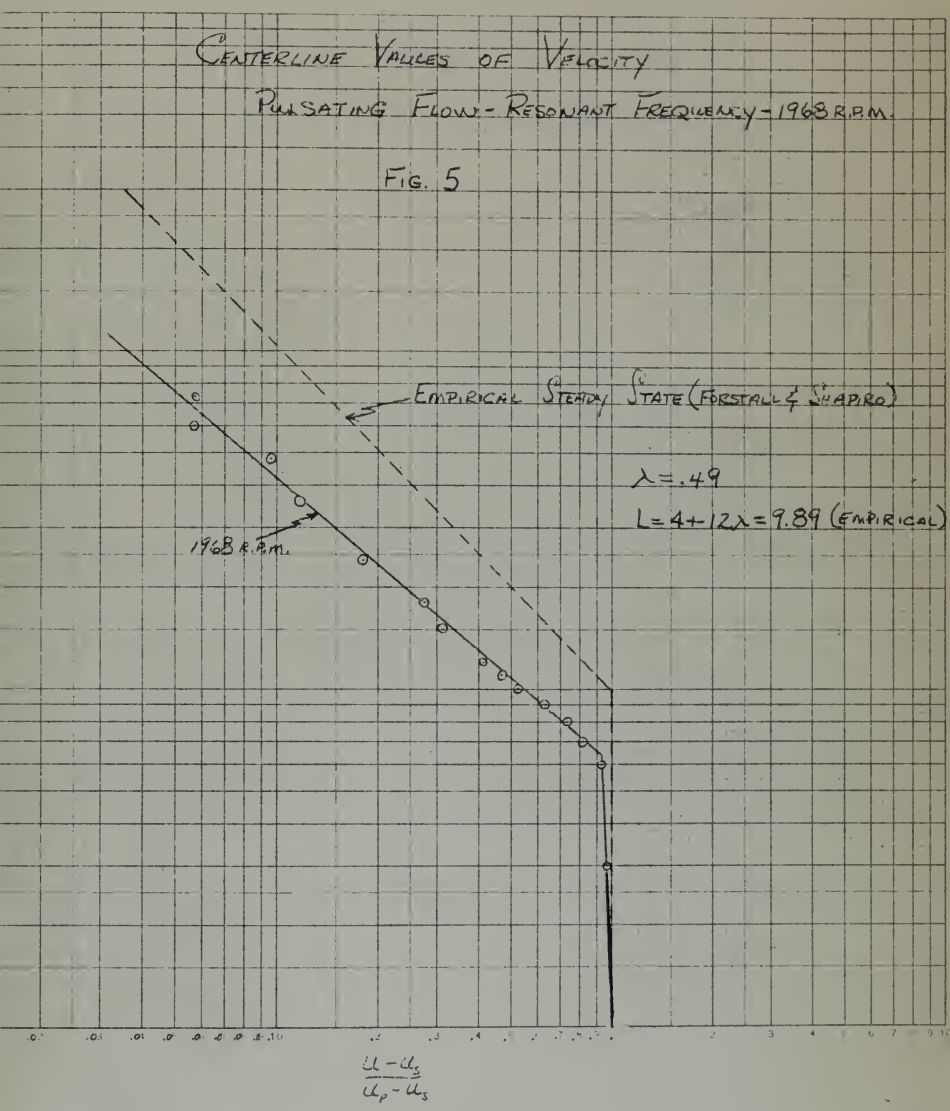

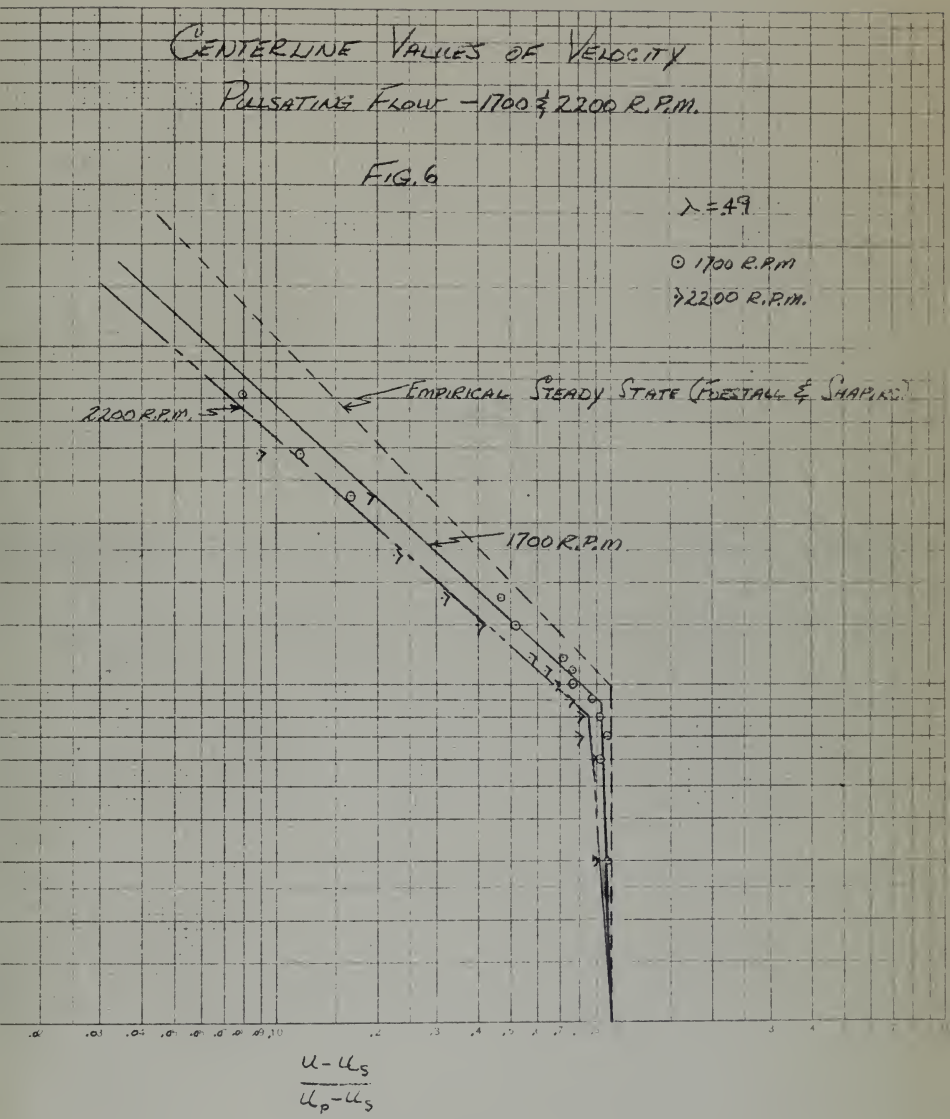
CENTERLINE VALUES OF VELOCITY
PULSATING FLOW - 1700 & 2200 R.P.M.
FIG. 6
λ = .49
⊙ 1700 R.P.M
2200 R.P.M.
EMPIRICAL STEADY STATE (FOSTAIL & SHAPIRO)
2200 R.P.M.
1700 R.P.M.
.01 .02 .03 .04 .05 .06 .08 .10 .2 .3 .4 .5 .6 .7 .8 1 2 3 4
$\frac{u - u_s}{u_p - u_s}$

# Centerline Value of Amplitude Velocity

## Resonant Frequency 1968 R.P.M.

Fig. 7

$$\frac{u_{a_x} - u_s}{u_a - u_s} = e^{-.032 \frac{x}{D}}$$

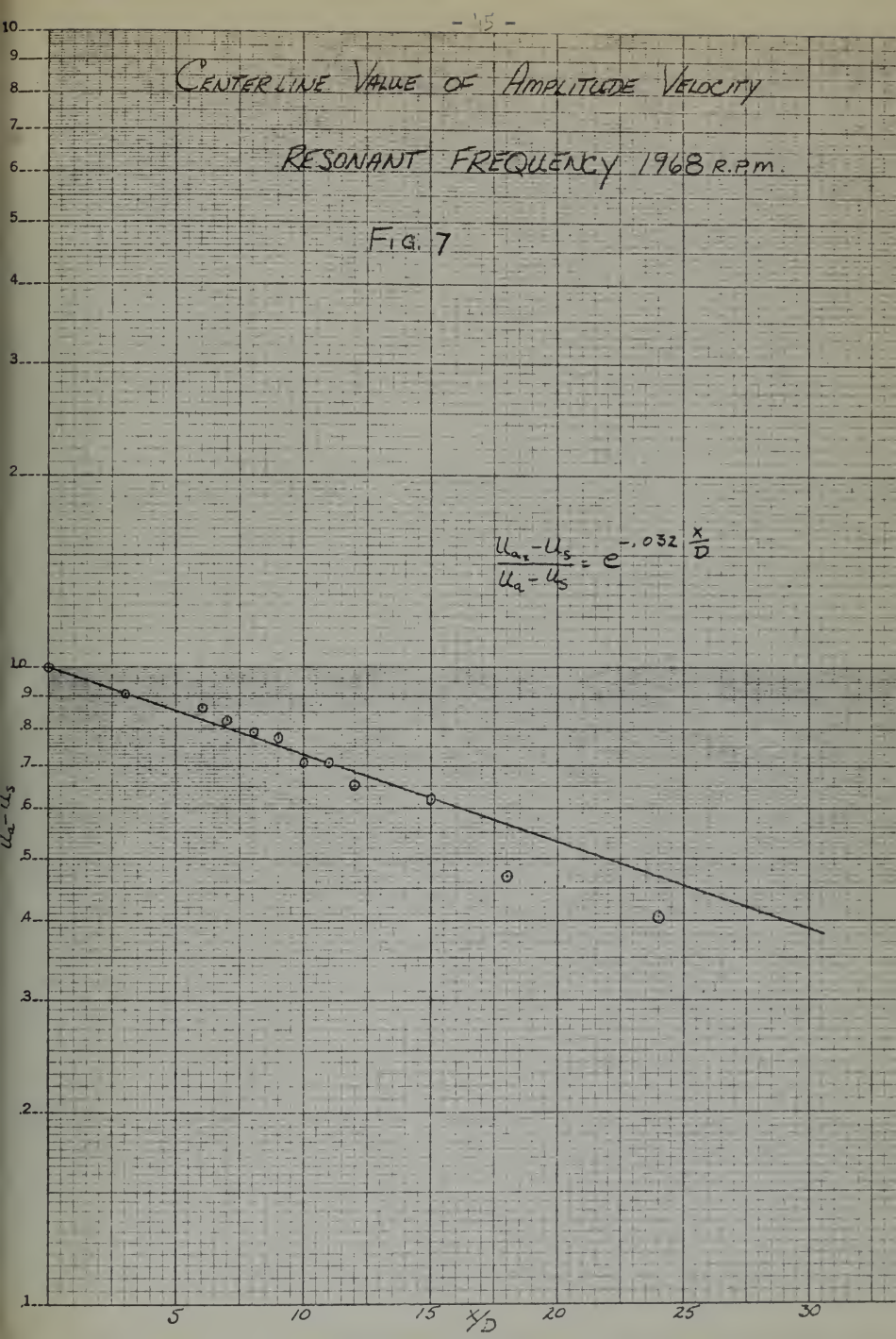

# Centerline Value of Amplitude Velocity

## For 1700 & 2200 R.P.M. Frequencies

Fig. 8

$$\frac{u_{a_x} - u_s}{u_a - u_s} = e^{-.051 \frac{x}{D}}$$

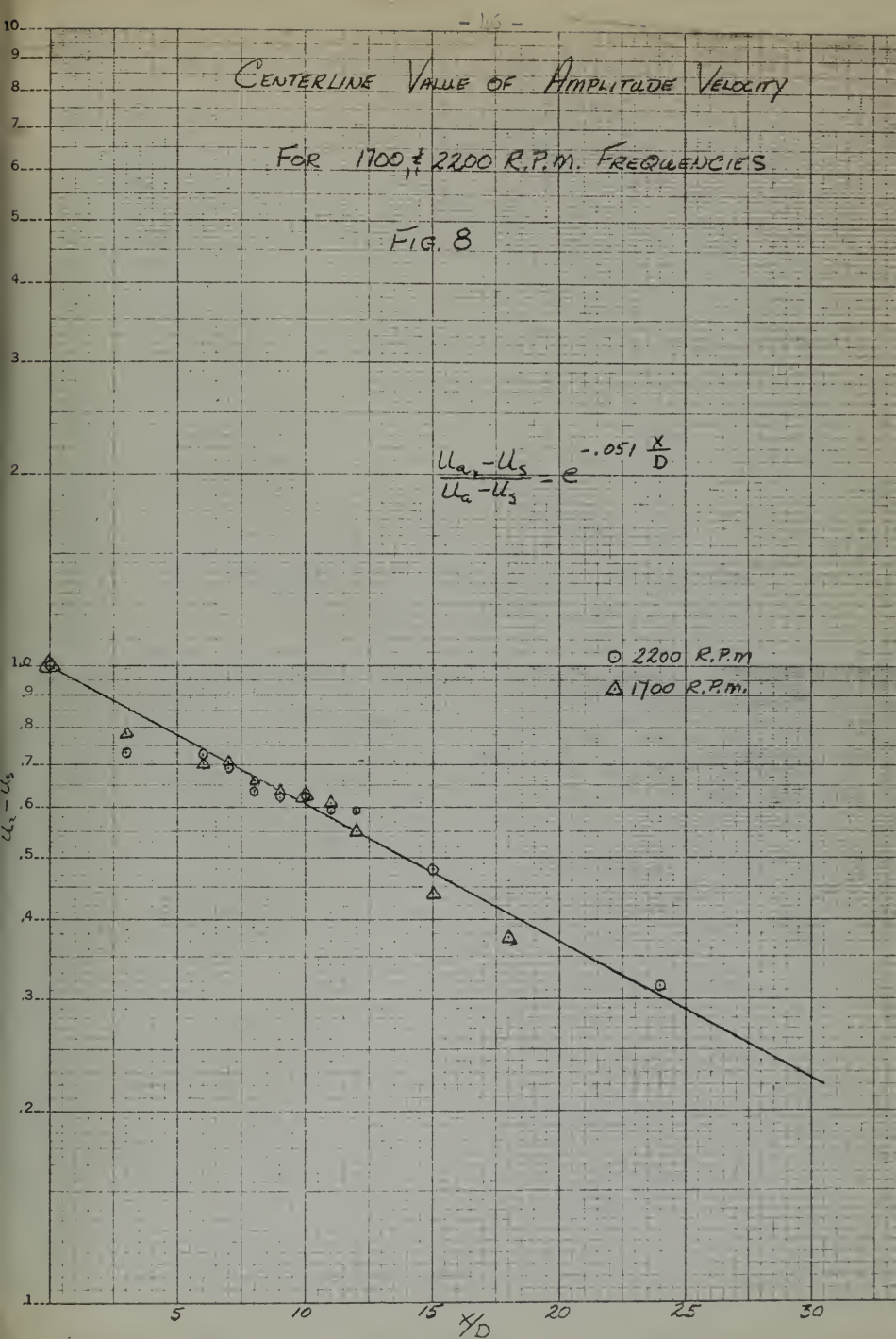

# Normalized Velocity Profile

## Steady State Run

Fig. 9

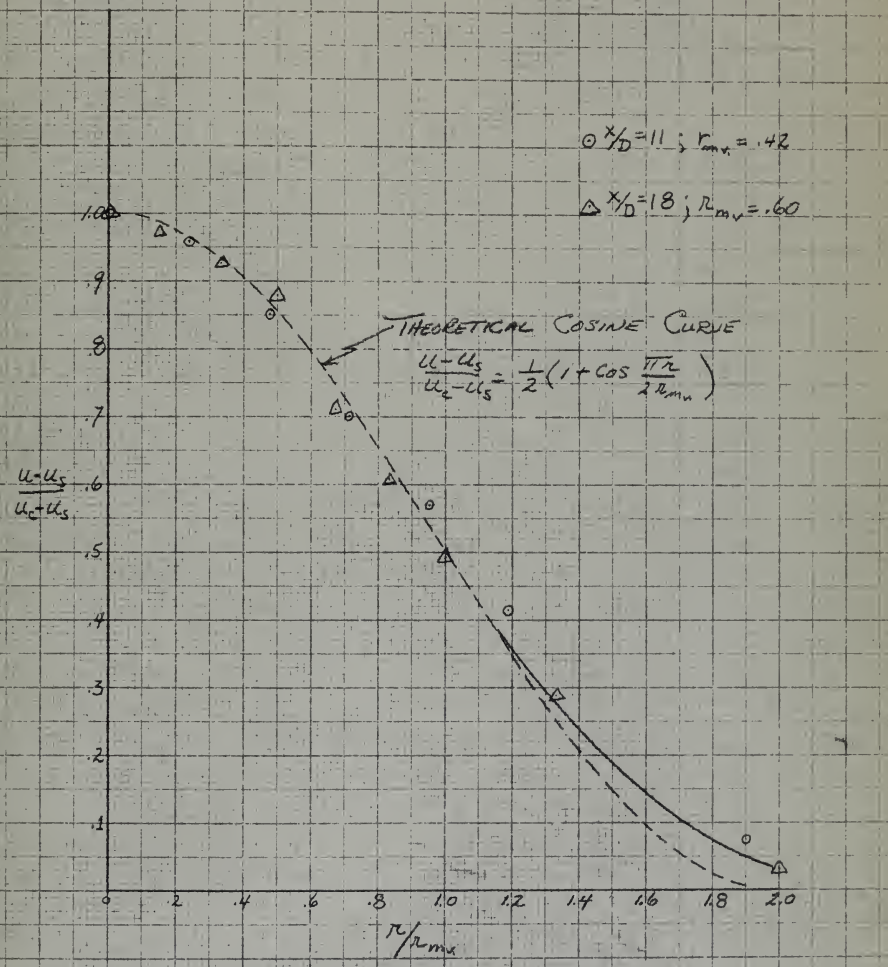

# NORMALIZED VELOCITY PROFILES

## PULSATING RUNS

FIG. 10

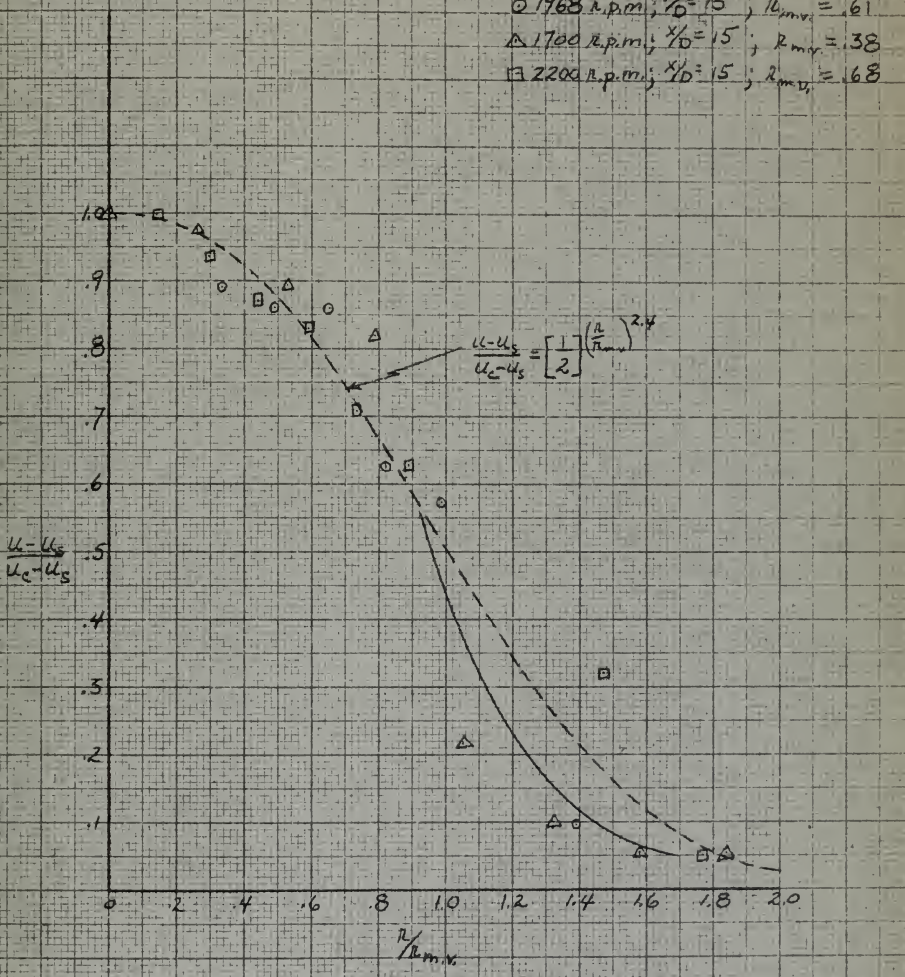

# Normalized Velocity Profile

## Pulsating Runs

Fig. 11

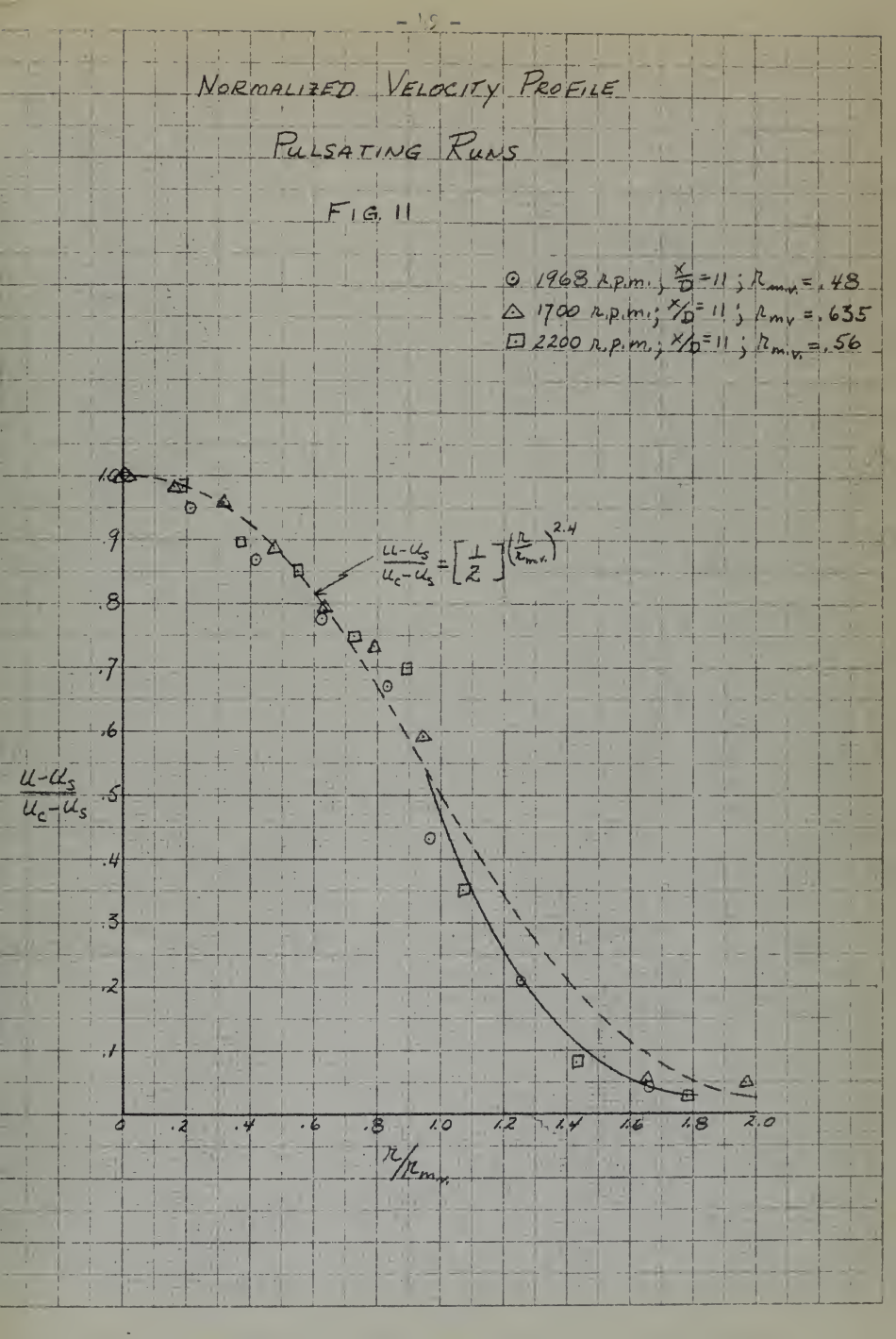

LATERAL VELOCITY PROFILE
STEADY FLOW

FIG. 12

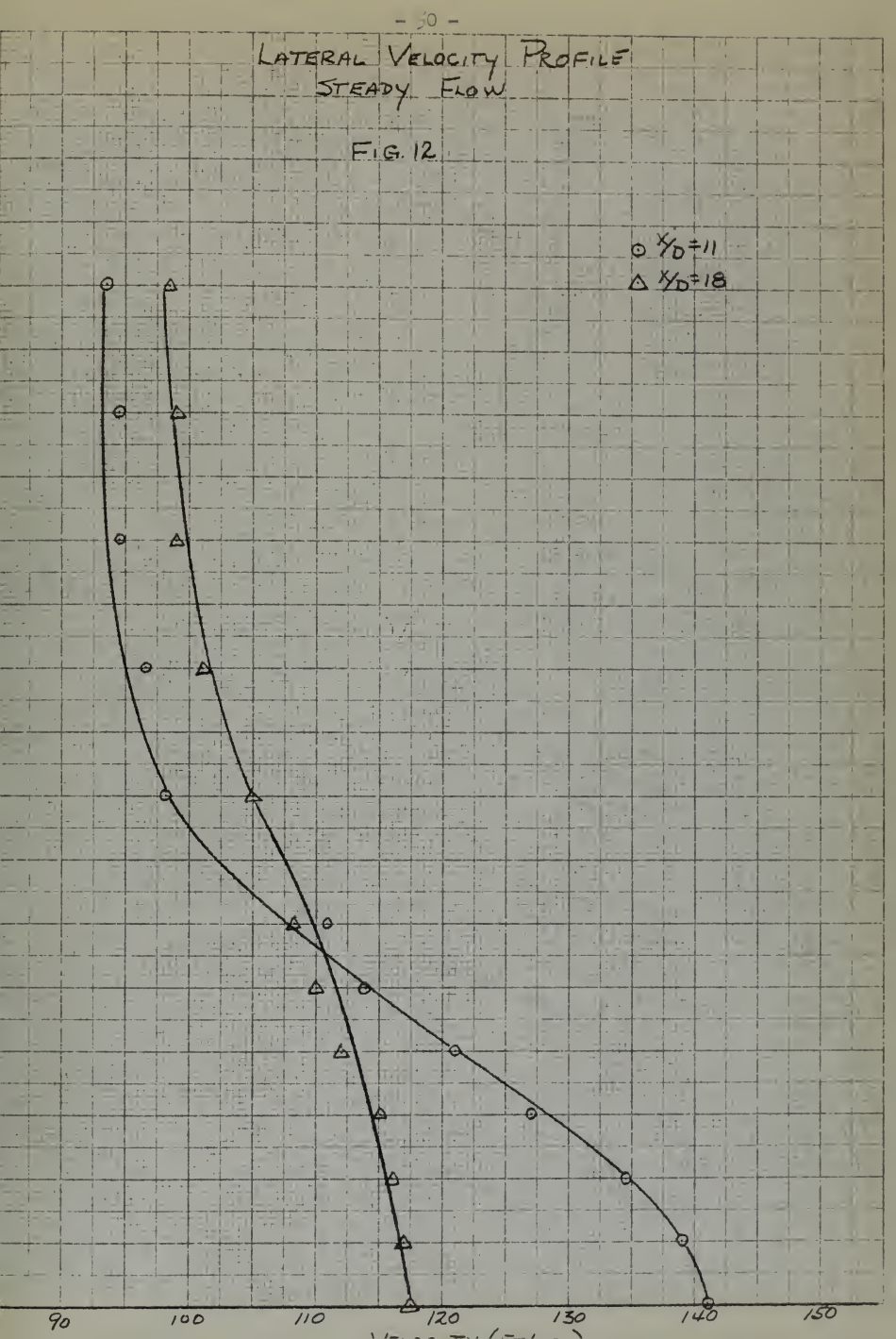

# LATERAL VELOCITY PROFILE

PULSATING FLOW - 1968 R.P.M.

FIG. 13

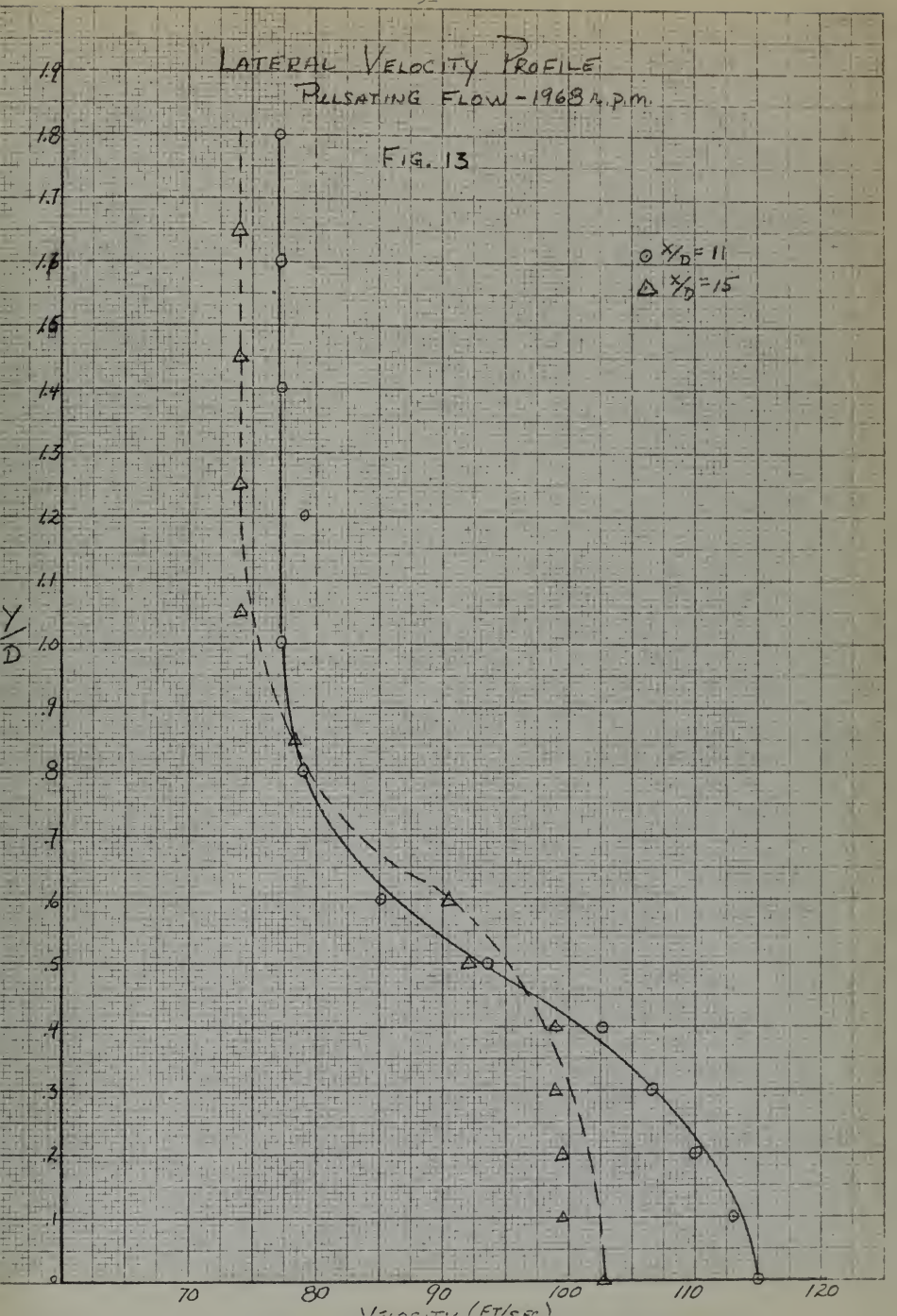

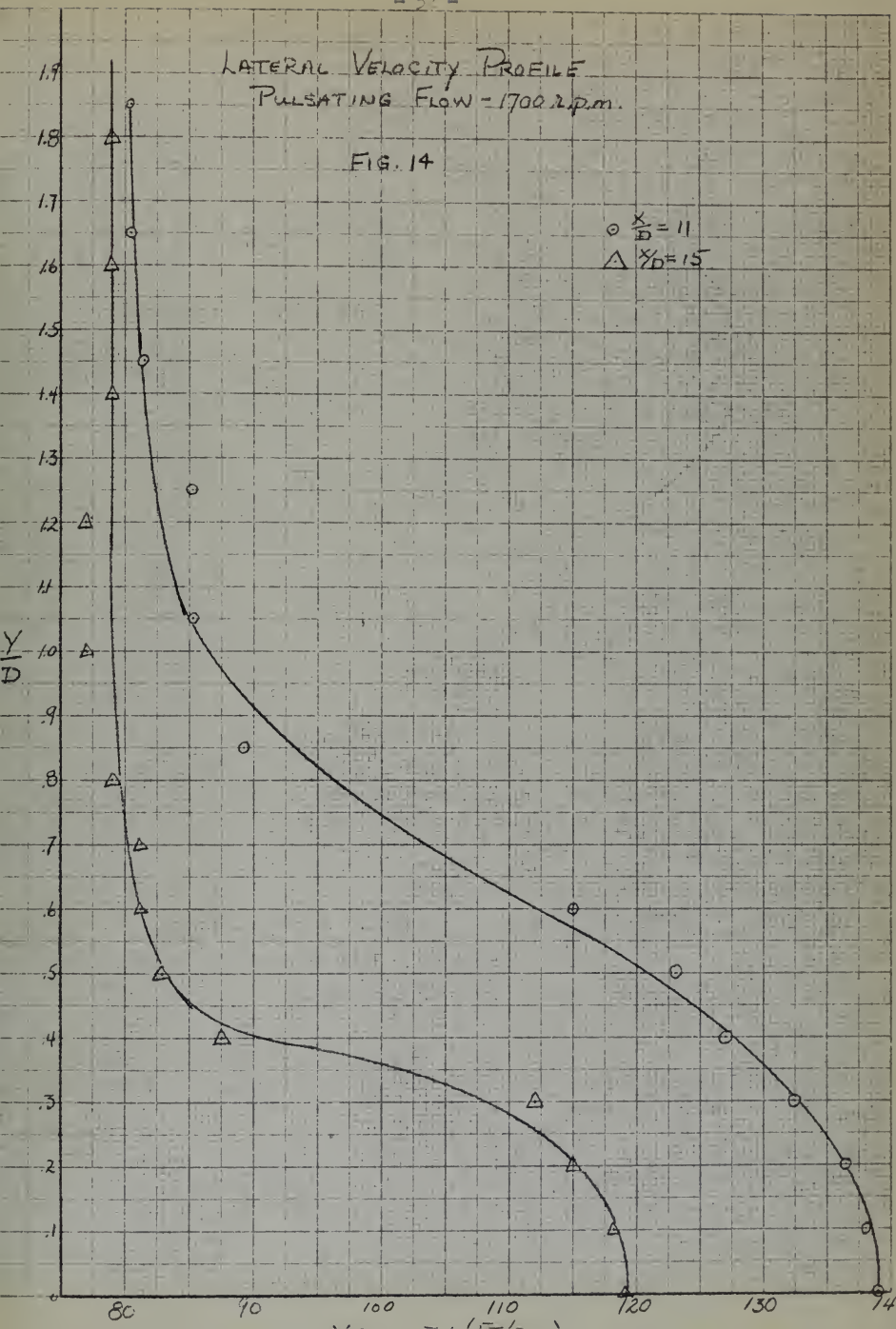
LATERAL VELOCITY PROFILE
PULSATING FLOW - 1700 2 p.m.
FIG. 14
○ X/D = 11
△ X/D = 15
Y/D
1.9
1.8
1.7
1.6
1.5
1.4
1.3
1.2
1.1
1.0
.9
.8
.7
.6
.5
.4
.3
.2
.1
0
80
90
100
110
120
130
140

# LATERAL VELOCITY PROFILE
## PULSATING FLOW - 2200 R.P.M.

FIG. 15

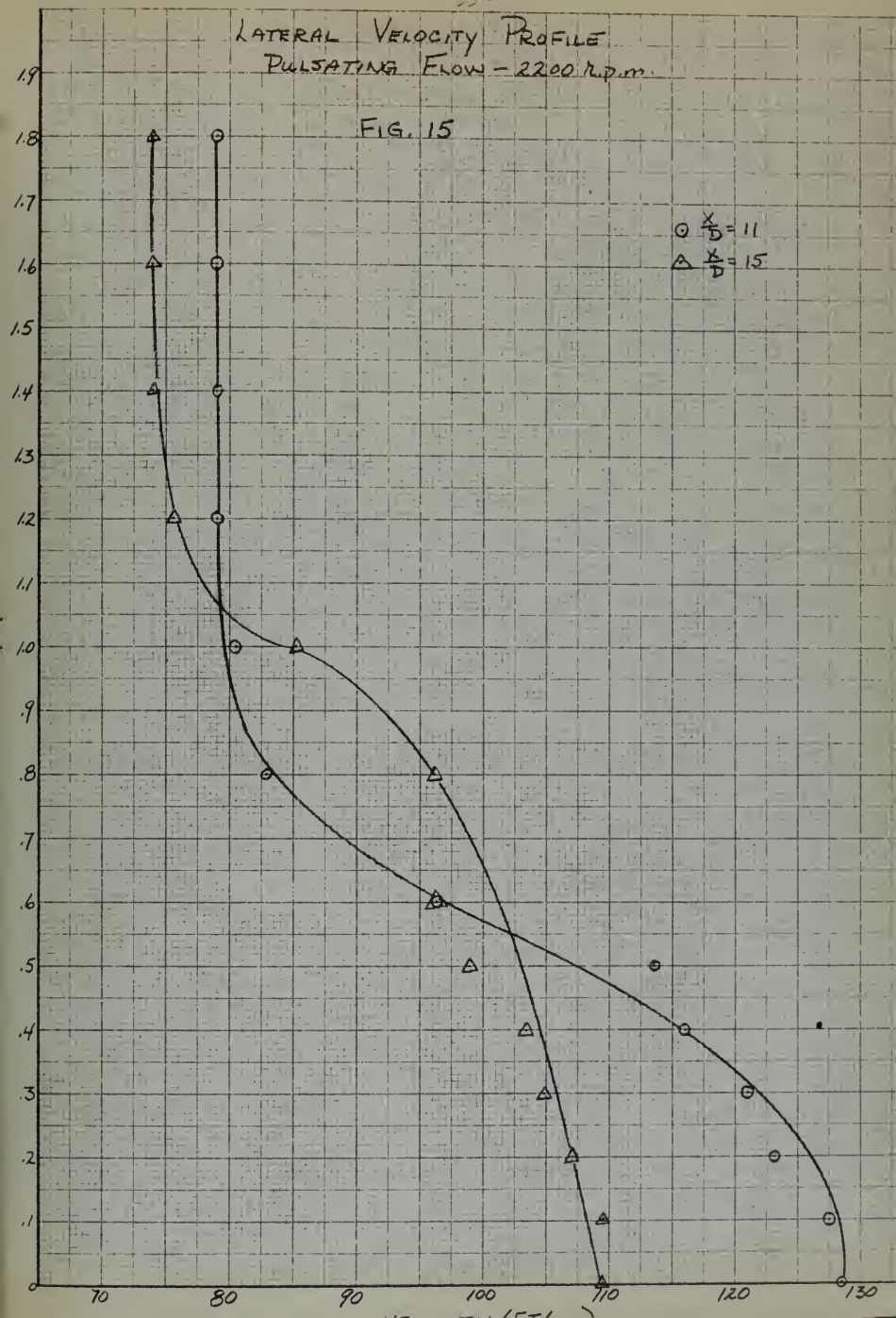

Thesis
R618 Robie
17334

An experimental analysis of the mixing of a pulsating air jet at varying frequencies in a steady air flow.